

I-mode: An H-mode Energy Confinement Regime with L-mode Particle Transport in Alcator C-Mod

D.G. Whyte¹, A.E. Hubbard¹, J.W. Hughes¹, B. Lipschultz¹, J.E. Rice¹, E.S. Marmor¹, M. Greenwald¹, I. Cziegler¹, A. Dominguez¹, T. Golfinopoulos¹, N. Howard¹, L. Lin¹, R.M. McDermott¹, M. Porkolab¹, M.L. Reinke¹, J. Terry¹, N. Tsujii¹, S. Wolfe¹, S. Wukitch¹, Y. Lin¹ and the Alcator C-Mod Team

¹MIT Plasma Science and Fusion Center, Cambridge, Massachusetts 02139, USA

e-mail contact of main author: whyte@psfc.mit.edu

Abstract. An improved energy confinement regime, I-mode is studied in Alcator C-Mod, a compact high-field divertor tokamak using Ion Cyclotron Range of Frequencies (ICRF) auxiliary heating. I-mode features an edge energy transport barrier without an accompanying particle barrier, leading to several performance benefits. H-mode energy confinement is obtained without core impurity accumulation, resulting in reduced impurity radiation with a high-Z metal wall and ICRF heating. I-mode has a stationary temperature pedestal with Edge Localized Modes (ELMs) typically absent, while plasma density is controlled using divertor cryopumping. I-mode is a confinement regime that appears distinct from both L-mode and H-mode, combining the most favorable elements of both. The I-mode regime is investigated predominately with ion ∇B drift away from the active X-point. The transition from L-mode to I-mode is primarily identified by the formation of a high temperature edge pedestal, while the edge density profile remains nearly identical to L-mode. Laser blowoff injection shows that I-mode core impurity confinement times are nearly identical with those in L-mode, despite the enhanced energy confinement. In addition a weakly coherent edge MHD mode is apparent at high frequency ~ 100 -300 kHz which appears to increase particle transport in the edge. In general the I-mode exhibits the strongest edge T pedestal and normalized energy confinement ($H_{98}>1$) at low q_{95} (<3.5) and high heating power ($P_{\text{heat}} > 4$ MW). I-mode significantly expands the operational space of ELM-free, stationary pedestals in C-Mod to $T_{\text{ped}} \sim 1$ keV and low collisionality $\nu_{\text{ped}}^* \sim 0.1$, as compared to EDA H-mode with $T_{\text{ped}} < 0.6$ keV, $\nu_{\text{ped}}^* > 1$.

1. Introduction

Optimized magnetic fusion energy (MFE) reactors face the seemingly contradictory requirements of high global energy confinement and low particle confinement. For net energy gain, a minimum level of energy confinement parameterized by $n\tau_E \sim 10^{21} \text{ m}^{-3} \text{ s}$ is required. However high global particle confinement time (τ_p) is not necessarily required since, unlike self-heating from alphas, the fuelling rate determining plasma density n is externally controlled. Simultaneously, overly high τ_p is usually undesirable due to the deleterious effects on fusion gain from accumulation of helium ash and impurity particles generated from plasma-wall interaction. Global confinement times are largely set by the edge pedestal [1] where an additional constraint is avoidance of peeling-ballooning instabilities which lead to MHD edge-localized modes (ELMs) and unacceptable transient heating of plasma-facing components [2]. In general therefore one desires *independent* understanding and control of the energy and particle transport channels in the core and pedestal regions in order to optimize MFE scenarios.

We explore an improved energy confinement regime ‘‘I-mode’’ [3,4] on Alcator C-Mod [5]. I-mode simultaneously features the desired properties of high-energy confinement of H-mode and the relatively poor particle confinement of low-confinement L-mode. The improved energy confinement results from the formation of an edge temperature pedestal, while density edge profiles remain essentially identical to those in L-mode. The pedestal is typically free of intermittent large ELMs yet plasma density is stationary, probably due to a high-frequency weakly coherent fluctuation contemporaneous with I-mode and observed in the pedestal region. I-mode demonstrates that the energy and particle transport channels in the pedestal

can be separated and isolated. A detailed description of the I-mode research result can be found in a recent publication [6].

2. Experimental Setup

Experiments were carried out on the compact, high-field Alcator C-Mod divertor tokamak [5]: major radius $R \sim 0.67$ m, minor radius $a \sim 0.22$ m and toroidal magnetic field $B_T < 8$ T (Fig. 1). C-Mod uses only high-Z bulk refractory metals of molybdenum and tungsten for plasma-facing components. Ion Cyclotron Range of Frequencies (ICRF) heating is the sole auxiliary heating method used in these experiments [7]. Fundamental hydrogen (H)-minority ICRF at 78-80.5 MHz up to 5.5 MW is used for central heating of deuterium (D) majority plasmas at typical magnetic field $B_T \sim 5.4$ T. In addition, the study includes a campaign at reduced B_T field (~ 3 -3.4 T) which primarily uses central ICRF H-minority 50 MHz heating, and some additional 80 MHz 2nd harmonic H-minority heating.

A typical C-Mod equilibrium shape for I-mode studies is shown in Fig. 1. The I-mode experiments mostly use an upper-single null divertor topology with “unfavorable” ion ∇B drift, i.e. with $B \times \nabla B$ pointed away from the primary X-point, which is known to increase significantly the auxiliary heating threshold to access H-mode as well as the threshold edge temperature [8,9]. Upper-null shapes can exploit strong divertor pumping for density control using the axisymmetric cryopump located there. I-mode has also been obtained in a few cases with the standard B direction, and thus $B \times \nabla B$ pointed towards the primary X-point. This I-mode was the result of using an atypical lower-null magnetic geometry for C-Mod (green dashed line, Fig. 1) with low upper triangularity, high lower triangularity and small X-point clearance to the inner divertor. Several key C-Mod diagnostic [10] locations are also shown in Fig. 1.

The C-Mod experimental campaign has identified and examined ~ 100 I-mode timeslices. A wide variety of heating power, plasma parameters and topologies has been explored: total heating power $P_{ICRF} + P_{ohmic} = P_{tot} \sim 1.3$ -5.7 MW, $B_T \sim 3$ -6 T, plasma current $I_p \sim 0.7$ -1.3 MA, $q_{95} \sim 2.5$ - 5, plasma elongation $\kappa \sim 1.5$ - 1.78, primary divertor triangularity $\delta \sim 0.3$ - 0.85, and average $\delta \sim 0.35$ -0.6. Although experiments were carried out through a campaign where boronization films were applied for plasma performance [11], none of the I-mode experimental days used boronization immediately preceding the experiment. Wall conditions were therefore variable and, in contrast to EDA H-modes [11], apparently not critical.

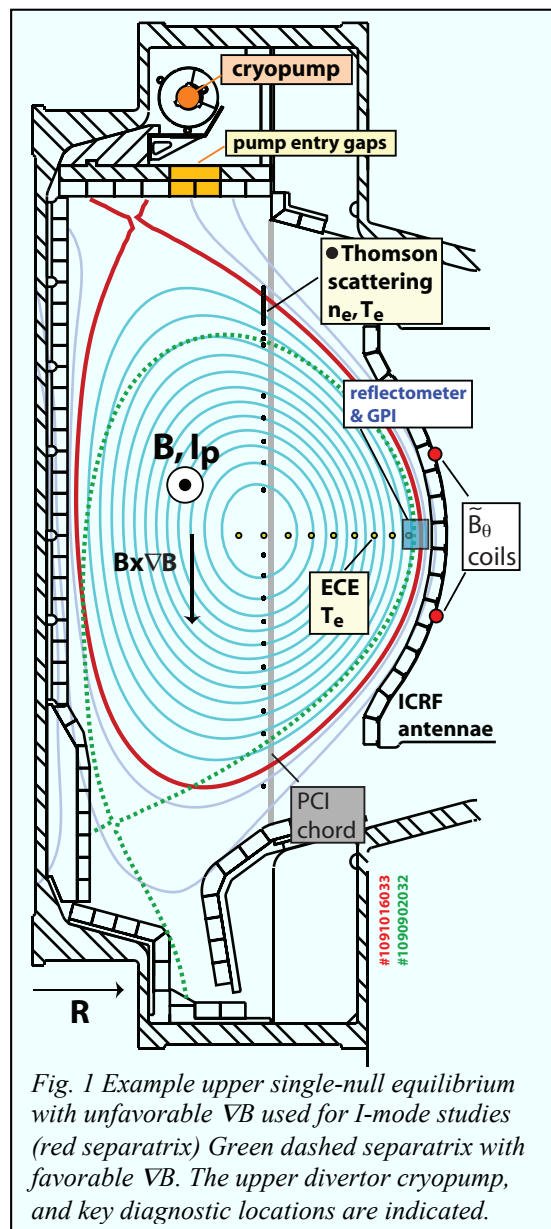


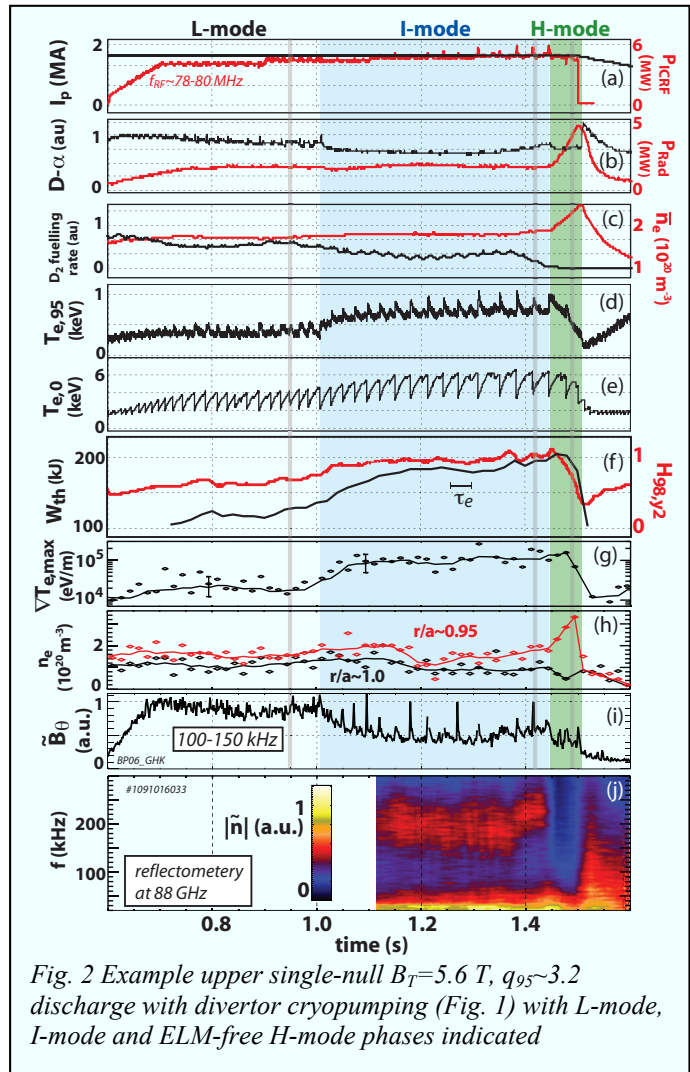
Fig. 1 Example upper single-null equilibrium with unfavorable ∇B used for I-mode studies (red separatrix) Green dashed separatrix with favorable ∇B . The upper divertor cryopump, and key diagnostic locations are indicated.

3. Experimental Results

In defining a confinement regime it is necessary to establish identifying features that make it distinct from standard L-mode confinement. Previous studies [3,4] showed that the I-mode was obtained in heating power ramps prior to H-mode, but featured neither a sudden D- α reduction nor a noticeable increase in density, making identification of the transition from L-mode to I-mode problematic based only on the standard L-H transition criteria. To avoid circular logic it is unacceptable to identify a transition in confinement regime solely by its confinement quality factor (H).

Exploration of I-mode over a wider parameter space on C-Mod has shown that distinct transitions from L-mode to I-mode indeed exist and can be clearly identified in most cases. In particular L-I transitions become very distinct on C-Mod in discharges with low $q_{95} < 3.5$ and high heating power ($P_{ICRF} > 3$ MW), an example of which is shown in Fig. 2. The discharge also features a transition to ELM-free H-mode for comparison.

The L-I transition is most clearly identified by the rapid increase in pedestal temperature ($T_{e,95}$) from L-mode values, simultaneous with the power pulse from a sawtooth crash (Fig 2d-e). In contrast to the edge temperature response to the sawtooth heat pulses in the preceding L-mode, $T_{e,95}$ does not decay at the L-I transition but is instead maintained, and even increases further, following the barrier formation. Through stiff core temperature profiles [1] the core temperature and stored energy increase as a result of the higher edge T_e . A confinement quality factor commensurate with H-mode, $H_{98,y2} \sim 1$ is obtained and maintained for more than 10 energy confinement times. However there is no noticeable change in the core density. The external fuelling rate (Fig. 2c, set by a feedback loop for density control with cryopumping) decreases gradually throughout the shot with its average value $\sim 30\%$ lower in I-mode than L-mode, yet active density control is maintained. The radiated power fraction (P_{rad}/P_{tot}) in I-mode tends to be relatively small and constant, varying between $P_{rad}/P_{tot} \sim 0.25 - 0.4$. At the transition to ELM-free H-mode the density and P_{rad} rise rapidly and uncontrollably (Fig. 2). Although RF heating power is constant, the subsequent decrease of conducted power to the pedestal/edge region due to core radiation from high-Z impurities, together with the increase in n_e , rapidly degrades the edge pedestal temperature and $H_{98,y2}$ decreases to ~ 0.5 . These issues of transient ELM-free H-mode performance at low q_{95} and impurity accumulation with an uncoated high-Z wall have been previously documented on C-Mod [11,12]. The evolution of the edge pedestal profiles is shown in Fig. 2g-h and Fig. 3. A large T_e pedestal gradient is established



at the I-mode transition, and the T_e profile is comparable to that found in the H-mode. In contrast with H-mode, there is no significant change in the I-mode edge density or n_e gradient compared to L-mode. Only when a subsequent transition into the H-mode occurs, a clear density pedestal is formed. *It is this formation of an edge thermal transport barrier in the absence of an edge particle transport barrier which is the key feature of I-mode.*

There are also marked changes in edge fluctuations at the transitions as shown in Fig. 2i-j. At the transition to I-mode there is a general decrease in low-frequency (~ 25 - 150 kHz) broadband density/magnetic fluctuations (Fig. 2i), while simultaneously a weakly coherent density/magnetic fluctuation exists at higher frequencies (Fig. 2j). This is reminiscent of the quasi-coherent mode of EDA H-mode [12] but appears at higher frequency and is significantly broader in frequency. At the transition to H-mode the weakly coherent mode (WCM) promptly disappears, along with a general sharp reduction in broadband fluctuations.

Based on multi-frequency reflectometry the WCM shown in Fig. 2 only exists between the 88 GHz and 110 GHz cutoffs, i.e. the 110 GHz reflectometer channel (not shown) does not detect the WCM. This observation squarely places the WCM in the I-mode T_e pedestal region between $0.9 < r/a < 1.0$ (Fig. 3b shows the densities associated with the cutoff frequencies).

Based on these observations the present criteria for the identification of an I-mode are that it:

- 1) Must show the formation of an edge T_e pedestal, either abruptly or gradually, without a significant change in the edge density profile as compared to L-mode,
- 2) Shows the appearance of a high frequency (> 100 kHz) weakly coherent magnetic/density mode (WCM) with an accompanying reduction in broadband fluctuations below the WCM frequency,
- 3) Must *not* show the signatures of an H-mode transition, namely an abrupt (< 1 ms) and sharp decrease in $D-\alpha$ along with a positive break-in-slope of the core density,

In addition to these three criteria, it is often observed that I-mode transitions show a break-in-slope of radiated power, stored energy and/or $D-\alpha$ that can also aid in identification of transitions (although this is not used as a primary criterion due to the inconsistency of these breaks).

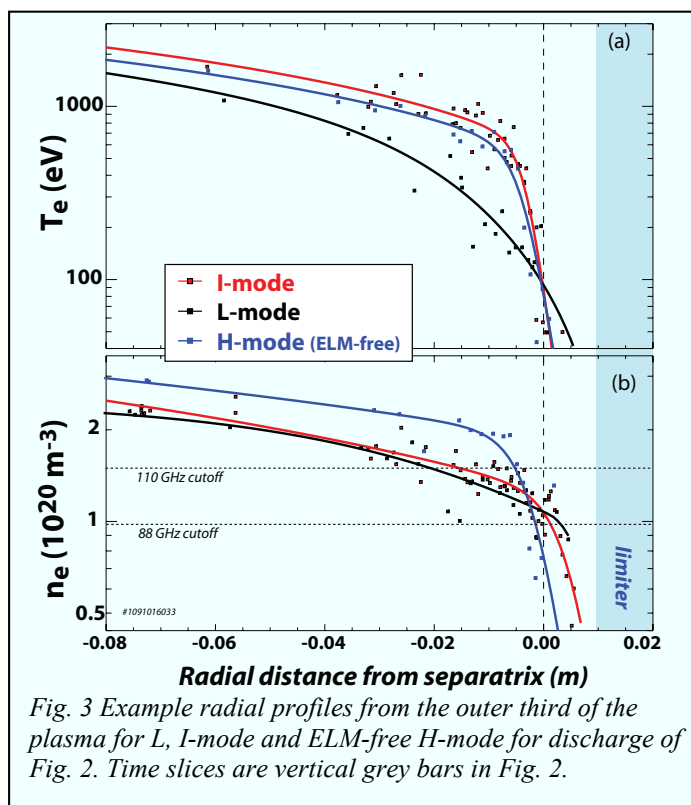


Fig. 3 Example radial profiles from the outer third of the plasma for L, I-mode and ELM-free H-mode for discharge of Fig. 2. Time slices are vertical grey bars in Fig. 2.

Fig. 4 shows that in general the required heating power ($P_{\text{loss}} \equiv P_{\text{tot}} - dW/dt$) to trigger a sudden transition to I-mode overlaps well with the range of heating power to trigger H-mode (except as noted, all discharges have unfavorable ∇B). Fig. 4a examines the power requirements to trigger L-I and I-H transitions established through small-range B_T/I_p scans at fixed ICRF heating frequencies. It has been found that the threshold P_{loss} for I and H mode transitions organizes well to q_{95} (although the 50 MHz, low B_T results of Fig. 4a show that there is a B_T dependence as well). The ratio of measured L-I and I-H threshold power to the widely used H-mode threshold power scaling $P_{\text{LH,scaling}}$ [13] is shown in Fig. 4b. The ratio $P_{\text{loss}}/P_{\text{LH,scaling}}$ is greater than unity as

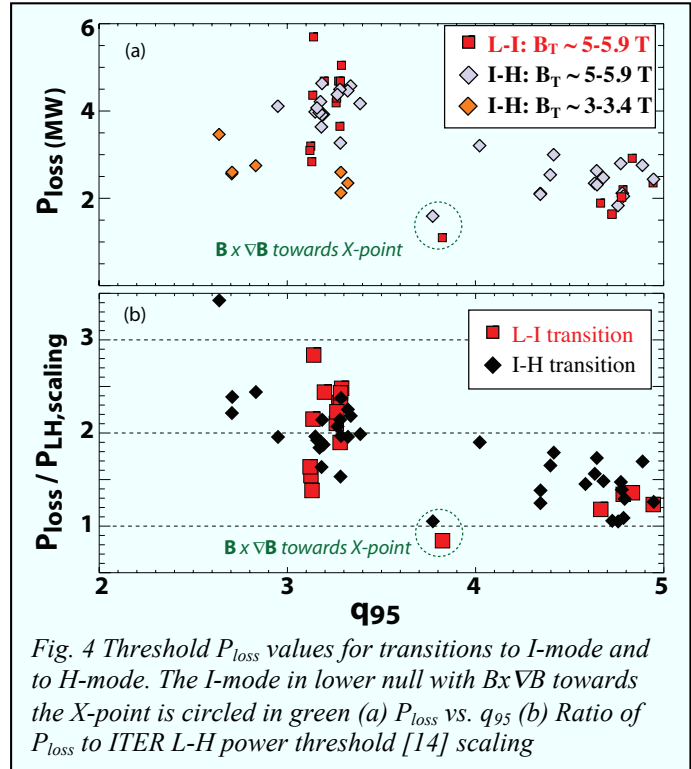


Fig. 4 Threshold P_{loss} values for transitions to I-mode and to H-mode. The I-mode in lower null with $B \times \nabla B$ towards the X-point is circled in green (a) P_{loss} vs. q_{95} (b) Ratio of P_{loss} to ITER L-H power threshold [14] scaling

expected for unfavorable ∇B drift direction. However the approximately linear inverse q_{95} ($1/I_p$) dependence we find for the threshold power does not appear in the standard H-mode threshold scaling prediction [13] and therefore appears to be a feature unique to unfavorable ∇B drift topology. This leads to a strong dependence on q_{95} for the “normalized” power to access I- or H-mode, with $P_{\text{loss}}/P_{\text{LH,scaling}} \sim 1.5-2.5$ at $q_{95} \sim 3$ and $P_{\text{loss}}/P_{\text{LH,scaling}} \sim 1.25$ at $q_{95} \sim 4.5-5$. A noteworthy exception to these trends is the lower-null I-mode case with $B \times \nabla B$ towards the X-point which has a substantially lower I- and H-mode power threshold and closely follows the scaling prediction, i.e. $P_{\text{loss}}/P_{\text{LH,scaling}} \sim 1$.

I-mode has an energy confinement quality roughly consistent with predictions of standard H-mode scaling over a wide range of parameter space. The confinement quality factor, $H_{98,y2}$ of I-mode lies in a narrow range near one as shown in Fig. 5 versus total heating power and q_{95} . Note, however, that I-modes are *not* identified by $H_{98,y2}$. The general trend is of increasing H_{98} with total heating power. The notable exceptions to this trend are I-modes with atypical shape for I-mode, i.e. favorable ∇B drift or lower-single null shapes with reversed B, both which obtain high H_{98} at $P_{\text{tot}} \sim 2$ MW. This suggests that further increases in performance may be achievable. Also, the lower field I-mode cases have consistently lower H_{98} than at nominal field $B_T \sim 5.4$ T. Fig. 5b shows that $H_{98,y2} \sim 0.9-1.1$ can be obtained over a wide range of q_{95} with a greater tendency for consistently high $H_{98} \sim 1$ values at lower $q_{95} < 3.5$. This contrasts with EDA H-mode which is strongly favored by $q_{95} > 3.5$ [14]. The favorable ∇B drift I-mode again stands apart from this trend with $H_{98} \sim 1.1-1.2$ at intermediate $q_{95} \sim 3.8$.

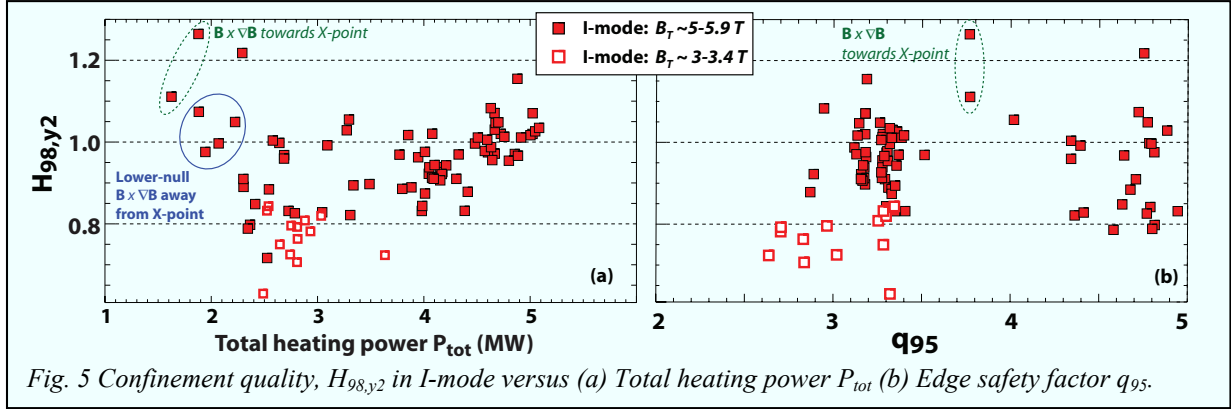


Fig. 5 Confinement quality, $H_{98,y2}$ in I-mode versus (a) Total heating power P_{tot} (b) Edge safety factor q_{95} .

Fig. 6 compares global impurity confinement time to H_{98} energy confinement quality for L-mode, I-mode and stationary EDA H-modes [15]. Impurity confinement time (τ_I) is obtained following laser ablation injection of calcium fluoride (CaF_2) films and the measurement of the central plasma Ca emission decay time with x-ray spectroscopy [16]. Ca injections into ELM-free H-modes have confinement times significantly longer than the duration of the H-mode (i.e. $> 0.2\text{-}0.5$ s) and so cannot be analyzed for τ_I . I-mode has energy confinement consistent with H-mode, but with the weak impurity particle confinement of L-mode ($\tau_I \sim 20\text{-}40$ ms $\sim \tau_e$). The I-mode impurity particle confinement time is considerably less than that found in stationary EDA H-modes. These observations are consistent with the fact that indicators of global particle confinement time are essentially unchanged between L- and I-mode: i.e. fuelling rate requirements (Fig. 2) and density profiles (Fig. 3) are not significantly modified when compared to the large changes in fuelling and density at H-mode transitions.

I-mode pedestal density and temperature profiles, including both core and edge Thomson scattering and ECE, have been fitted (e.g. Fig. 3) to a modified hyperbolic function conventionally used for H-mode pedestal analysis. These fits include timeslices from the I-mode campaign as well as example stationary EDA H-modes from earlier pedestal scaling studies [17] and recent ELMy H-modes, the latter two with favorable ∇B drift topology.

The I-mode discharges are clearly on a lower collisionality T vs. v^* “track” than H-mode, i.e. the I-mode collisionality is lower for a given pedestal temperature. Fig. 7 shows the pedestal electron temperature vs. pedestal neoclassical collisionality, v_{95}^*). I-mode significantly expands the C-Mod operational space of stationary ELM-free regimes: from the collisional ($v_{95}^* > 1$) L-mode/EDA regimes with $T_{ped} < 0.6$ keV to the collisionless ($v_{95}^* \sim 0.1$) I-mode with T_{ped} approaching 1 keV.

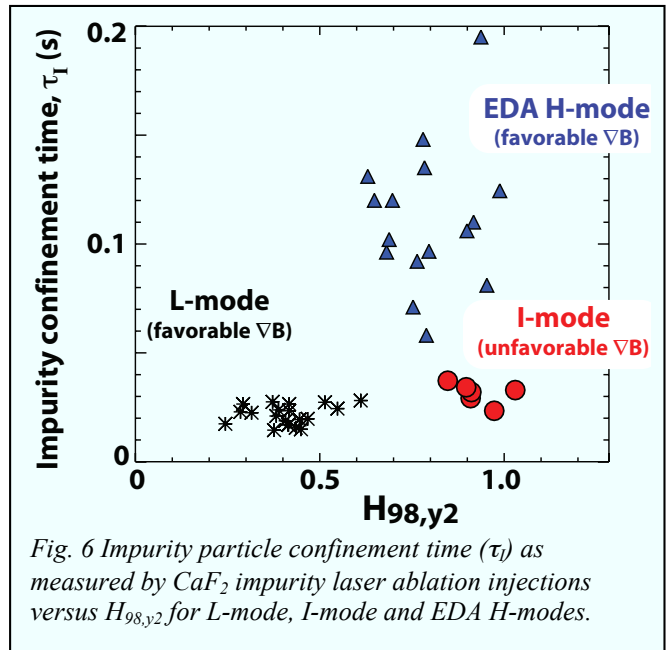


Fig. 6 Impurity particle confinement time (τ_I) as measured by CaF_2 impurity laser ablation injections versus $H_{98,y2}$ for L-mode, I-mode and EDA H-modes.

For completeness, it should be noted that small, infrequent ELMs have occasionally been seen in I-mode. These ELMs are almost always triggered by a sawtooth pulse (similar to I-H transition triggers). The ELMs are quite small in size with $\Delta T/T_{\text{ped}} \sim 5\text{-}10\%$, i.e. smaller than edge perturbations caused by the sawteeth. Stored energy loss from the ELM is small enough in magnitude so as to make its measurement difficult in the presence of sawtooth crashes. For the infrequent case of an ELM not triggered by a sawtooth crash we roughly estimate from magnetics and kinetic profiles: $\Delta W_{\text{ELM}}/W_{\text{th}} \sim 0.5\text{-}1.5\%$ and $\Delta W_{\text{ELM}}/W_{\text{ped}} \sim 2\text{-}5\%$. Given the pedestal collisionality $\nu_{\text{ped}}^* \sim 0.2$ in this case, we make a preliminary assessment that these belong in a “small” ELM category as compared to normalized ELM energy loss from other devices [18]. Whatever their characteristics, these ELMS play a minimal role in regulating core particle or impurity content during I-mode. To date we have not identified a particular operational condition(s) that causes these infrequent ELM; more often the I-mode phases are completely free of ELMs (e.g. Fig. 2).

4. Discussion

The study of I-mode has two important motivations: 1) understanding transport and threshold physics and 2) developing optimized operational scenarios.

Pertaining to the first motivation, I-mode is a self-organized plasma state like H-mode, but one in which the energy and particle transport channels are clearly separated. This feature makes I-mode a valuable tool in exploring the underlying transport, as well as the physics associated with the transition to high confinement modes. I-mode lacks a density pedestal, which obviously has important consequences for edge pressure profiles and the resulting self-consistent edge bootstrap currents important for stability. Along with the lack of ELMs, this suggests that I-mode is exploring a somewhat different (and interesting) part of the edge stability space than standard H-mode. Like the QCM of EDA H-mode, I-mode has a short wavelength, edge MHD mode (WCM) that appears to regulate particle transport. However the QCM favors high q_{95} and collisionality, while the WCM can manifest at low q_{95} and low collisionality. Taken together the observations above argue that I-mode has a different set of feedback mechanisms between the underlying turbulence, the profile/gradient plasma fields and accompanying MHD stability. The cross-correlation among the fluctuation fields is also likely to be different in I-mode in order to permit significant cross-field turbulent particle transport, yet highly suppressed energy transport, in a collisionless edge plasma.

Pertaining to the second motivation, I-mode exhibits operational scenario advantages that make it highly attractive. I-mode features a high temperature, low collisionality pedestal

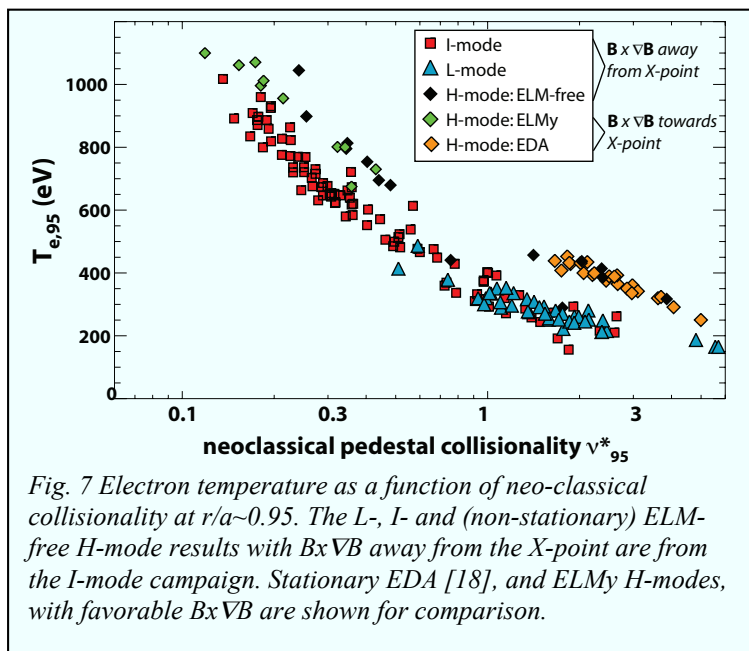


Fig. 7 Electron temperature as a function of neo-classical collisionality at $r/a \sim 0.95$. The L-, I- and (non-stationary) ELM-free H-mode results with $B \times vB$ away from the X-point are from the I-mode campaign. Stationary EDA [18], and ELMy H-modes, with favorable $B \times vB$ are shown for comparison.

without ELMs, a condition which will be required in ITER and other future large scale fusion devices. I-mode simultaneously provides impurity and density control in an ICRF-heated high-Z wall tokamak without the requirement of immediately preceding boronizations. In addition, power handling in the divertor should be greatly aided by a broader L-mode SOL profile (Fig. 3). A possible difficulty in exploiting I-mode in ITER is the high power generally required to trigger the L-I transition (Fig. 4). However it should be noted that in several individual cases, the threshold power is within <25% of the standard H-mode threshold scaling. It is premature to assess if ITER can access I-mode. But expanding access to I-mode at lower power densities, with a variety of fuelling techniques and with other magnetic topologies, would be valuable in determining its general applicability as an operational regime

5. Conclusions

An improved energy confinement regime, I-mode has been studied in the Alcator C-Mod tokamak. I-mode features an edge energy transport barrier without a strong accompanying particle barrier. To date I-mode has primarily been accessed in C-Mod with the following experimental conditions: upper-null topology with high upper triangularity and BxVB pointed *away* from the primary X-point, on axis H(D)-minority ICRH plasma heating and divertor cryopumping for density control. H-mode energy confinement is obtained without core impurity accumulation. As a result, I-mode has stationary and reduced impurity radiation as compared to H-modes previously obtained with a high-Z metal wall and ICRF heating. I-mode also features a stationary edge pedestal, which usually is completely free of ELMs. I-mode is a confinement regime that appears distinct from both L-mode and H-mode, both in its global performance and in its local pedestal and fluctuation characteristics.

Acknowledgments

This work was supported by U.S. DOE Cooperative Agreement DE-FC02-99ER54512

References

- [1] Greenwald, M., et al. 1997 *Nuclear Fusion* **37** 793
- [2] Loarte, A., et al. 2007 *Nuclear Fusion* **47** 203
- [3] McDermott, R.M., et al. 2009 *Physics of Plasmas* **16** 056103
- [4] Ryter, F., et al. 1998 *Plasma Physics and Controlled Fusion* **40** 725
- [5] Marmar, E.S., et al. 2007 *Fusion Science and Technology* **51** 261
- [6] Whyte, D.G. et al. 2010 *Nuclear Fusion* **50** 105005
- [7] Bonoli, P.T., et al. 2007 *Fusion Science and Technology* **51** 401
- [8] Hubbard, A.E., et al. 2007 *Physics of Plasmas* **14** 056109
- [9] ASDEX-team 1989 *Nuclear Fusion* **29** 1959
- [10] Basse, N.P., et al. 2007 *Fusion Science and Technology* **51** 476
- [11] Lipschultz, B., et al. 2006 *Physics of Plasmas* **13** 56117
- [12] Greenwald, M., et al. 1999 *Physics of Plasmas* **6** 1943
- [13] Martin, Y.R., Takizuka, T. 2008 *Journal of Physics: Conference Series* **123** 012033
- [14] Hughes, J.W., et al. 2007 *Fusion Science and Technology* **51** 317
- [15] Rice, J.E., et al. 2007 *Fusion Science and Technology* **51** 357
- [16] Howard, N., Greenwald, M., Rice, J.E. 2010 "Characterization of impurity confinement on Alcator C-Mod using a multi-pulse laser blow-off system," submitted to *Review Scientific Instruments*
- [17] Hughes, J.W. et al. 2002 *Physics of Plasmas* **9** 3019
- [18] Loarte, A., et al. 2003 *Plasma Physics and Controlled Fusion* **45** 1549